

PGE₂ mediates EGFR internalization and nuclear translocation *via* caveolin endocytosis promoting its transcriptional activity and proliferation in human NSCLC cells

Lorenzo Bazzani^{1,2}, Sandra Donnini¹, Antonio Giachetti¹, Gerhard Christofori² and Marina Ziche¹

¹Department of Life Sciences, University of Siena, Siena, Italy

²Department of Biomedicine, University of Basel, Basel, Switzerland

Correspondence to: Marina Ziche, **email:** marina.ziche@unisi.it

Keywords: nuclear EGFR; PGE₂; clathrin and caveolin endocytosis; gene transcription; cell proliferation

Received: September 13, 2017 **Accepted:** February 10, 2018 **Epub:** February 15, 2018 **Published:** March 13, 2018

Copyright: Bazzani et al. This is an open-access article distributed under the terms of the Creative Commons Attribution License 3.0 (CC BY 3.0), which permits unrestricted use, distribution, and reproduction in any medium, provided the original author and source are credited.

ABSTRACT

Prostaglandin E₂ (PGE₂) contributes to tumor progression by promoting cancer cell growth, invasion and by creating a favorable pro-tumor microenvironment. PGE₂ has been reported to transactivate and internalize into the nucleus receptor tyrosine kinases such as Epidermal growth factor receptor (EGFR), thereby supporting tumor progression. Here we demonstrate that in non-small cell lung carcinoma (NSCLC) cells, PGE₂ induces EGFR nuclear translocation *via* different dynamin-dependent endocytic pathways, promotes the formation of an EGFR-STAT3 complex, affects nuclear EGFR target gene expression and mediates tumor cell proliferation. Indeed, we find that PGE₂ induces EGFR internalization and consequent nuclear import through Clathrin- and Caveolin-mediated endocytosis and through the interaction of EGFR with Importin β1. Within the nucleus, EGFR forms a complex with STAT3, an event blocked by ablation of Clathrin Heavy Chain or Caveolin-1. The combination of EGF and PGE₂ prolongs nuclear EGFR transcriptional activity manifested by the upregulation of *CCND1*, *PTGS2*, *MYC* and *NOS2* mRNA levels and potentiates nuclear EGFR-induced NSCLC cell proliferation. Additionally, NSCLC patients with high expression of a nuclear EGFR gene signature display shorter survival times than those with low expression, thus showing a putative correlation between nuclear EGFR and poor prognosis in NSCLC. Together, our findings indicate a complex mechanism underlying PGE₂-induced EGF/EGFR signaling and transcriptional control, which plays a key role in cancer progression.

INTRODUCTION

Prostaglandin E₂ (PGE₂) promotes tumor growth by inducing an inflammatory microenvironment, in autocrine or paracrine fashion, through the activation of 4 receptor subtypes: EP1, EP2, EP3, EP4 [1–3]. Besides the plethora of biological processes evoked by prostanoids through the binding to their receptors, PGE₂ reportedly interacts with various receptor tyrosine kinase (RTK) in a process termed transactivation [4], exemplified by EGFR activation

in several cancer cell types [5–10]. Upon binding with PGE₂, EP receptors trigger different downstream effectors including PKA, PKC, SRC and PI3K to mediate EGFR activation [11].

We have recently reported that PGE₂ induces EGFR internalization and nuclear translocation supporting tumor progression in non-small cell lung cancer (NSCLC) cells [12]. Indeed, we have shown that PGE₂-induced EGFR transactivation promotes its nuclear import and the subsequent SRC/ADAMs-mediated autocrine and/or

paracrine release of soluble cell-surface EGF like ligands, an event that culminates in EGFR-mediated transcriptional activities and enhanced tumor cell proliferation [12].

Numerous reports have shown that EGFR recruits proteins and transduces signaling pathways also inside the cell [13, 14]. Upon ligand binding, EGFR undergoes either Clathrin-mediated endocytosis (CME) or Clathrin-independent endocytosis (CIE), including lipid-raft dependent routes, such as Caveolin-mediated endocytosis and macropinocytosis [15]. EGFR is mainly internalized via Clathrin-mediated endocytosis [16], yet saturation of Clathrin or stimulation with different ligands has been shown to induce alternative routes of internalization, including Caveolin-mediated endocytosis and macropinocytosis [17–19].

In light of the above mentioned PGE₂-induced EGFR nuclear translocation, we have tested which internalization routes might be involved in EGFR nuclear shuttling in NSCLC cells and whether PGE₂ could sustain nuclear EGFR transcriptional activity and tumor progression. Here, we describe the internalization mechanisms by which PGE₂ regulates EGFR nuclear translocation and affects tumor gene expression and cancer cell proliferation.

RESULTS

Inhibition of the large GTPase dynamin blocks PGE₂-induced EGFR nuclear import

EGFR is internalized either via Clathrin-mediated endocytosis or via Caveolin-mediated endocytosis and macropinocytosis [16–18, 20]. In order to discriminate between the EGFR endocytic modalities induced by PGE₂, we used pharmacological inhibitors of these pathways employing A549 and GLC82 NSCLC cells. Stimulation with either EGF (25 ng/ml) or PGE₂ (1 μM) induced EGFR nuclear translocation with a peak at 10 and 60 min, respectively (Figure 1A and Supplementary Figure 1A). Clathrin- and Caveolin-mediated endocytosis are both dependent on the activity of the large guanosine 5'-triphosphatase (GTPase) dynamin [21], whereas macropinocytosis is susceptible to Na⁺/H⁺ exchange inhibitors, such as amiloride [22]. Thus, A549 cells were pre-treated with a specific dynamin inhibitor, Dynasore (DYN), or with a Na⁺/H⁺ exchange inhibitor, 5-(N-Ethyl-N-isopropyl) amiloride (EIPA) before challenge with EGF (Figure 1B) or PGE₂ (Figure 1C). In EGF or PGE₂-treated cells, DYN markedly reduced EGFR nuclear accumulation, whereas no effect was observed with EIPA (Figure 1B and 1C). Similar results were obtained with GLC82 cells (Supplementary Figure 1B). Immunofluorescence staining followed by confocal microscopy analysis showed that in control conditions and in NSCLC cells treated with DYN or EIPA alone, EGFR was confined to the cell membrane (Figure 1D). DYN

pretreatment of NSCLC cells blocked the nuclear import of EGFR induced by either EGF (10 min) or PGE₂ (60 min), whereas EIPA treatment failed to affect the EGFR internalization and nuclear translocation process (Figure 1D). The results indicate that dynamin-dependent Clathrin- and Caveolin-mediated endocytosis might be involved in EGF and PGE₂-induced EGFR nuclear translocation.

PGE₂ promotes EGFR internalization and nuclear translocation via Clathrin- and Caveolin-mediated endocytosis

To further dissect the endocytic mechanism, we used a genetic approach to inhibit Clathrin and Caveolin-mediated endocytosis by performing knockdown of both Clathrin Heavy Chain, the major component of Clathrin-coated vesicles [23] and knockdown of Caveolin-1, the primary constituent of Caveolae [24]. A549 and GLC82 cells were transiently transfected with siRNA against Clathrin Heavy Chain (siClathrin) or against Caveolin-1 (siCaveolin-1) or with a non-targeting siRNA (siControl) for 48 hours and then treated with EGF (10 min) or PGE₂ (60 min). Clathrin knockdown abrogated EGFR nuclear translocation induced by both EGF and PGE₂, while Caveolin-1 ablation suppressed only PGE₂-induced EGFR nuclear translocation (Figure 2A). The efficient knockdown of Clathrin Heavy chain and Caveolin-1 expression was confirmed by immunoblotting (Figure 2B). A similar phenotype was observed in GLC82 cells. Clathrin Heavy chain knockdown hindered both EGF and PGE₂-mediated EGFR nuclear translocation. Conversely, knockdown of Caveolin-1 impaired only PGE₂-mediated EGFR nuclear accumulation (Supplementary Figure 2A and 2B). Immunofluorescence confocal microscopy analysis confirmed the strong reduction of EGFR internalization and nuclear translocation in Clathrin Heavy chain knockdown setting (Figure 2C middle panels) and the dependency on Caveolin-mediated endocytosis of PGE₂-induced EGFR nuclear translocation (Figure 2C lower panels). Knockdown of both Clathrin Heavy chain and Caveolin-1, impaired PGE₂ activity to a similar extent as si-Clathrin Heavy chain or si-Caveolin-1 alone, suggesting that the prostanoid appears to promote nuclear EGFR translocation with two independent signaling pathways (Supplementary Figure 3A). The efficient knockdown of Clathrin Heavy chain and Caveolin-1 expression was confirmed by immunoblotting (Supplementary Figure 3B).

To validate the results on Caveolin-mediated endocytosis, we employed Methyl- β -cyclodextrin (M β CD), a cyclic oligomer of glucopyranoside that inhibits cholesterol-dependent Caveolae-mediated endocytosis, by reversibly extracting the steroid out of lipid rafts [25]. In A549 cells, incubated with increasing concentration of M β CD (1, 5, 10 mM) before EGF or PGE₂ treatment, we found no effect on EGF-mediated

EGFR nuclear translocation (Figure 2D), whereas a reduced EGFR nuclear accumulation was observed after PGE₂ stimulation, demonstrating that Caveolin-mediated endocytosis plays a role in PGE₂-induced EGFR nuclear translocation (Figure 2E). Taken together, these findings

underline the prominent role of Clathrin-mediated endocytosis in EGFR internalization, yet the data also demonstrates that Caveolin-mediated endocytosis is an alternative endocytic route for PGE₂-induced nuclear translocation of EGFR.

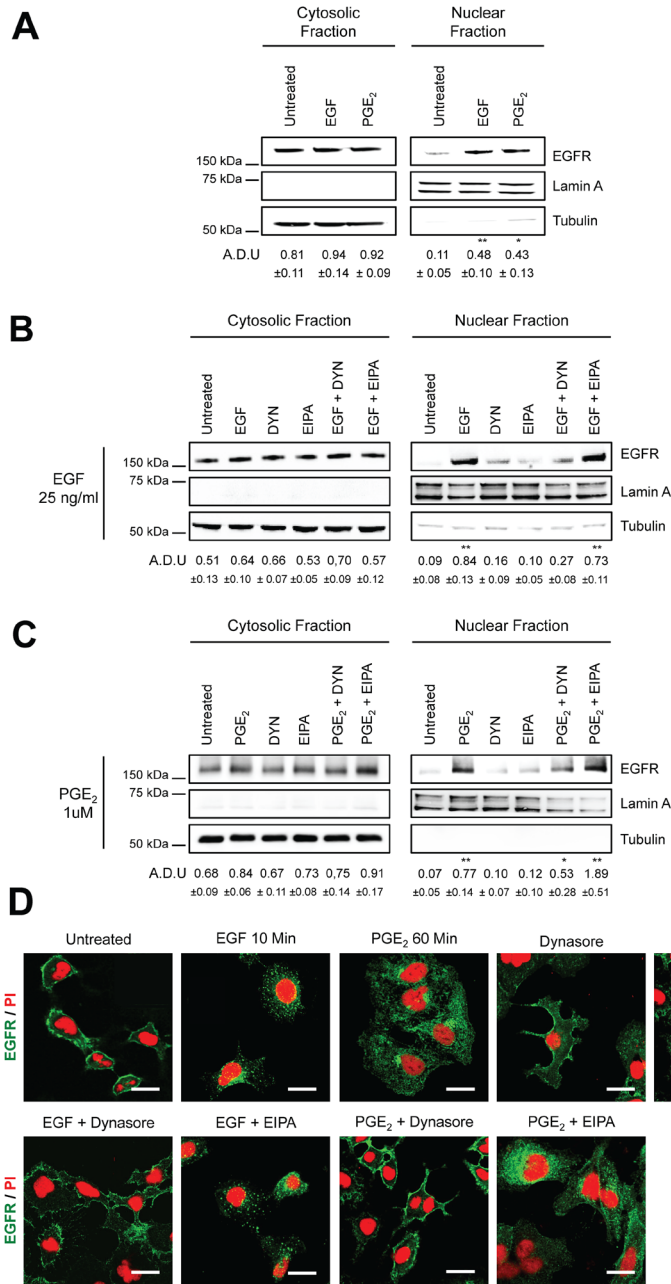


Figure 1: Dynamin inhibition blocks EGF- and PGE₂-induced EGFR nuclear translocation. Immunoblotting analysis of EGFR expression in cytosolic and nuclear fraction in overnight starved A549 (A–C). Cells were exposed to 10 min to 25ng/ml EGF or to 60 min 1μM PGE₂ (A). A549 cells were starved overnight and then treated for 30 min with dynasore 80μM (DYN) or 100μM 5-(N-Ethyl-N-isopropyl)amiloride (EIPA) before challenge with 25ng/ml EGF or 1μM PGE₂ for 10 and 60 min respectively (B, C). Tubulin and Lamin A were used as loading control for cytosolic and nuclear fraction. Immunoblotting quantification was expressed in A.D.U. (arbitrary density unit) and as mean ± SD. *p < 0.05, **p < 0.01 vs Ctrl. EGFR in the cytoplasmic and nuclear fractions was normalized to Tubulin or Lamin A respectively. (D) Confocal analysis of EGFR localization in A549 treated as described above and then fixed with paraformaldehyde and stained with anti-EGFR (green) and Propidium Iodide (red). Confocal images were captured in the middle section of the nuclei with Zeiss LSM700 microscope using 63x objective, scale bars 20 μm. The experiments were performed three times.

a knockdown of Importin β 1 by transfecting A549 cells with siRNA against Importin β 1 or with a non-targeting siRNA (siControl). Exposure to EGF or PGE₂ of Importin β 1-silenced cells dramatically reduced EGFR nuclear translocation upon both EGF and PGE₂ treatments (Figure 3A). Downregulation of Importin β 1 was assessed by immunoblotting analysis (Figure 3B). The role of Importin β 1 was further validated by immunofluorescence confocal microscopy analysis. In Importin β 1-ablated cells, EGFR was still mobilized from cell membrane upon both EGF and PGE₂ treatment, however, nuclear localization was abrogated (Figure 3C). These results demonstrate that, as for EGF, PGE₂-mediated EGFR nuclear translocation requires Importin β 1.

PGE₂ induces the formation of an EGFR-STAT3 complex in the nucleus

As EGFR lacks a DNA binding domain, nuclear EGFR exerts its transcriptional functions via the interaction with various transcription factors [29]. Among the transcriptional target genes, nuclear EGFR is recruited to the ATRS motif of the cyclin D1 (*CCND1*), inducible nitric oxide synthase (*NOS2*), c-Myc (*MYC*) and COX-2 (*PTGS2*) promoters through its interaction with several transcription factors, including STAT3 [30–34]. We previously observed that *CCND1*, *PTGS2*, *MYC* and *NOS2* were highly modulated by PGE₂-induced nuclear EGFR [12]. Thus, we first investigated whether PGE₂ promoted STAT3 phosphorylation and then the role of JAK in mediating this signaling pathway. In A549 cells exposed to PGE₂ from 5 to 60 min, the prostanoid induced STAT3 activation in a time-dependent manner with a peak at 30 min (Figure 4A). Next, 30 minutes pre-treatment of NSCLC cells with a JAK inhibitor, Ruxolitinib at 10 μ M, as well as with a STAT3 inhibitor, STAT3 inhibitor VII at 10 μ M, significantly reduced the PGE₂ effect (Figure 4B).

Notably, PGE₂ promoted EGFR-STAT3 protein–protein interaction as determined by co-immunoprecipitation experiments. A549 cells were exposed to EGF (10 min) or PGE₂ (60 min), and EGFR was immunoprecipitated and the potential binding of STAT3 to EGFR was analyzed by immunoblotting. Upon EGF and PGE₂ treatment, STAT3, either in its non-phosphorylated or phosphorylated condition, efficiently co-immunoprecipitated with EGFR (Figure 4C, 4D). In order to show whether EGFR and STAT3 form a complex inside the nucleus, we performed cell fractionation followed by immunoprecipitation. We observed that EGFR was bound to STAT3 in the nucleus suggesting a possible mechanism for the transcriptional activation of the *PTGS2*, *MYC* and *NOS2* genes (Figure 4E). To assess the contribution of the two above-described internalization routes on EGFR transcriptional activity, we transiently transfected A549 and GLC82 cells with siRNAs against Clathrin Heavy Chain (siClathrin) or against Caveolin-1

(siCaveolin-1) or with a non-targeting siRNA (siControl) for 48 hours before treatment with EGF (10 min) or PGE₂ (60 min) (Figure 4F and Supplementary Figure 4A). In Clathrin-ablated A549 cells exposed to EGF or PGE₂, the formation of an EGFR-STAT3 complex was significantly reduced, confirming the central role of Clathrin-mediated endocytosis in EGFR internalization (Figure 4F and Supplementary Figure 4A middle panels). However, Caveolin-1 silencing affected PGE₂-induced EGFR-STAT3 association, corroborating the ability of the prostanoid to use an alternative endocytic pathway (Figure 4F and Supplementary Figure 4A right panels). The knockdown efficiency of Clathrin Heavy chain and Caveolin-1 was confirmed by immunoblotting analysis blot (Figure 4G and Supplementary Figure 4B). The simultaneous knockdown of both Clathrin Heavy chain and Caveolin-1 did not appear to modify PGE₂ efficacy on EGFR-STAT3 nuclear association, compared to knockdown of Clathrin Heavy chain or Caveolin-1 alone (Supplementary Figure 5A). The knockdown efficiency of Clathrin Heavy chain and Caveolin-1 was confirmed by immunoblotting analysis blot (Supplementary Figure 5B). Taken together, our data demonstrate that PGE₂ induces the formation of an EGFR-STAT3 nuclear complex and that different endocytic mechanisms contribute to the association of EGFR with STAT3.

Combination of EGF and PGE₂ promotes the transcription of nuclear EGFR target genes up to 8 hours

We previously reported that EGF and PGE₂ alone induced the transcription of the nuclear EGFR-target genes *CCND1*, *PTGS2*, *MYC* and *NOS2*, with a maximal activation at 2 h and 4 h, respectively [12]. To assess the effect of a combination of EGF and PGE₂ on the expression of these nuclear EGFR transcriptional target genes, A549 EGFR-knockout cells were generated by CRISPR/Cas9 (Figure 5A). Two cell clones, genetically deficient for EGFR expression (EGFR $-/-$ #1 and #2), were transfected with plasmid constructs either encoding for wild type EGFR (WT) or EGFR mutated in its nuclear localization sequence (NLSm12 and dNLS) [32]. In NSCLC cells transfected with NLSm12 or dNLS constructs, EGFR nuclear translocation, promoted by the challenge with EGF or PGE₂, was markedly reduced compared to cells transfected with WT EGFR or to parental cells (Figure 5B, 5C) [12].

A549 cells transfected with constructs encoding for WT and mutant EGFR showed similar level of EGFR expression (Figure 5D). Quantitative real-time PCR (qRT-PCR) analysis was performed in parental and modified A549 cells (Figure 6) exposed to EGF or PGE₂ or a combination in a time course up to 12 or 18 hours. In parental and EGFR $-/-$ A549 cells bearing EGFR WT plasmid, EGF promoted the expression of nuclear EGFR

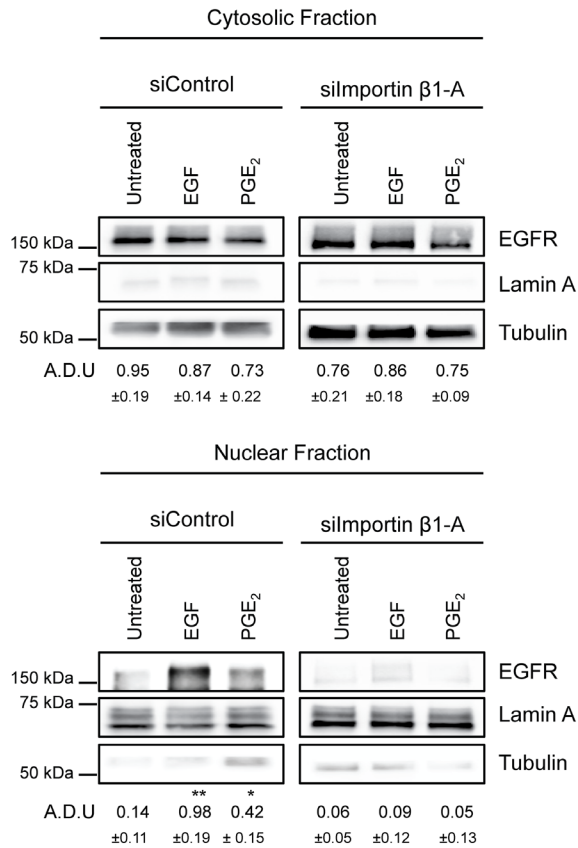
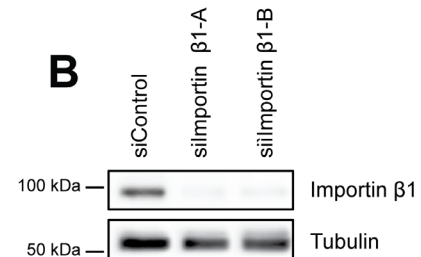
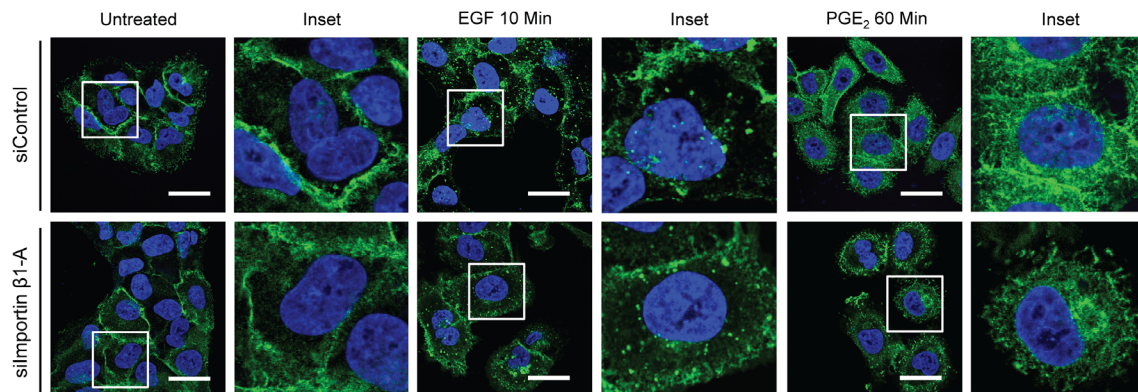
A**B****C**

Figure 3: Importin β 1 is required for EGFR nuclear translocation. (A) A549 cells were transfected with siRNA control or siRNA against Importin β 1 for 48h. Next, cells were serum starved overnight and exposed to 25ng/ml EGF for 10 min or to 1 μ M PGE₂ for 60 min. EGFR level in cytoplasmic and nuclear fraction was assessed using immunoblot with indicated antibodies. (B) Knockdown efficiency was verified via western blot with Importin β 1 antibody, Tubulin was used as loading control. Similar data were obtained with siImportin β 1-B. Immunoblotting quantification was expressed in A.D.U. (arbitrary density unit) and as mean \pm SD. * p < 0.05, ** p < 0.01 vs Ctrl. EGFR in the cytoplasmic and nuclear fractions was normalized to Tubulin or Lamin A respectively. (C) A549 cells were transfected as indicated above. After that cells were fixed and stained for EGFR (green) and DAPI (blue). Confocal images were captured in the middle section of the nuclei with Leica SP5 confocal using 63x objective, scale bars 20 μ m. Panel shows representative picture for each experimental condition. Boxed areas are shown in detail in the inset. The experiments were performed three times.

target genes with a peak at 2 h and declined to baseline at 4-8 h, whereas PGE₂ mimicked the EGF effect on target genes with a peak at 4 h and declined toward the baseline at 8-12 h. The combination of EGF and PGE₂ recapitulated the outcome of both individual treatments, yet showing a fostered transcription of target genes up to

8 h (Figure 6). Similar results were observed in GLC82 cells (Supplementary Figure 6). The statistical analysis is presented in Tables 1–2 and Supplementary Table 1 for A549 and GLC82 cells, respectively.

Next, we investigated the prognostic role of the nuclear EGFR gene signature. We exploited the Lung

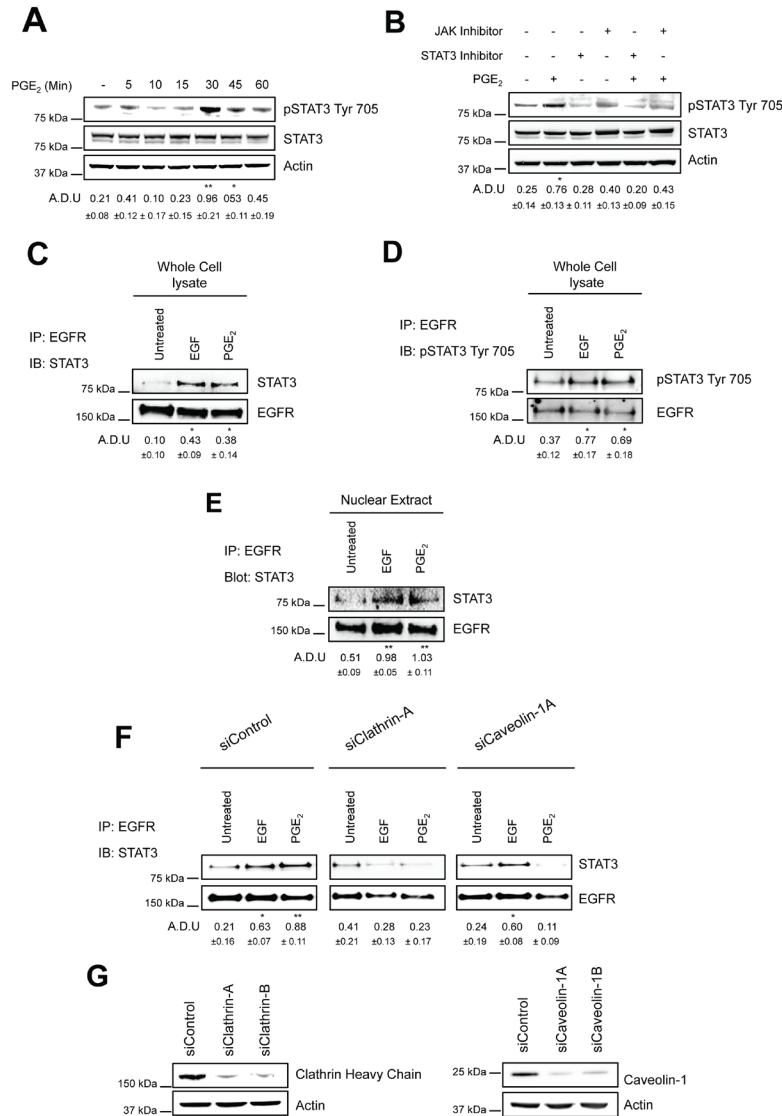


Figure 4: PGE₂ induces the formation of EGFR-STAT3 complex into the nucleus. (A) Immunoblotting analysis of STAT3 phosphorylation on Tyr 705 in overnight starved A549 exposed to 1 μM PGE₂ for 5–60 min. (B) Immunoblotting analysis of STAT3 phosphorylation on Tyr 705 in A549 exposed for 30 min to 1 μM PGE₂, with or without pre-incubation with JAK inhibitor, Ruxolitinib (10 μM), or STAT3 inhibitor, STAT3 inhibitor VII, for 30 min. Actin was used as loading control. (C–E) A549 cells were overnight starved and then exposed to 25ng/ml EGF or 1μM PGE₂ for 10 and 60 min respectively. Whole cell lysate (C–D) and nuclear extract (E) were subjected to immunoprecipitation with anti-EGFR antibody and analyzed by immunoblotting with anti-STAT3 or anti-phosphoSTAT3 Tyr 705 antibodies. (F) A549 cells were transfected with siRNA Control or siRNA against Clathrin Heavy Chain or against Caveolin-1 for 24 h. Cells were then serum starved overnight and treated with 25ng/ml EGF for 10 min or 1μM PGE₂ for 60 min. Whole cell lysates were subjected to immunoprecipitation with anti-EGFR antibody and analyzed by immunoblotting with anti-STAT3 antibody. (G) Knockdown efficiency was verified via western blot with Clathrin heavy chain and Caveolin-1 antibodies, actin was used as loading control. Data are shown only for siClathrin-A and siCaveolin-1A, similar data were obtained with siClathrin-B and siCaveolin-1B. Immunoblotting quantification was expressed in A.D.U. (arbitrary density unit) and as mean ± SD. *p < 0.05, **p < 0.01 vs Ctrl. In panel A and B, pSTAT3 Tyr 705 was normalized to STAT3. In panels C–F, STAT3 was normalized to EGFR. The experiments were performed three times.

Adenocarcinoma TCGA study, including 230 tumor samples with mRNA expression data (RNA Seq V2) by cBioPortal for Cancer Genomics data sets [35, 36]. Alterations, which consists in mRNA upregulation of the nuclear EGFR target genes were found in 51 of 230 patients (22%) as shown in percentages of total samples as follows: *CCND1* (10%), *PTGS2* (3%), *MYC* (8%) and *NOS2* (1,7%) (Figure 7). Kaplan–Meier analysis for predicted overall patient survival indicated that cases with

alteration of nuclear EGFR gene signature had shorter survival times than those with no alteration (log-Rank test, $P < 0.0777$), the median survival time being reduced from 46.7 to 35.5 months (Figure 7). Notably, in the group of patients with mRNA upregulation of nuclear EGFR target genes, the deceased patients were 16 on 44 (36.3%), whereas in the group of patients without mRNA upregulation of nuclear EGFR target genes the deceased ones were 47 on 159 (29.5%). These data indicate a trend,

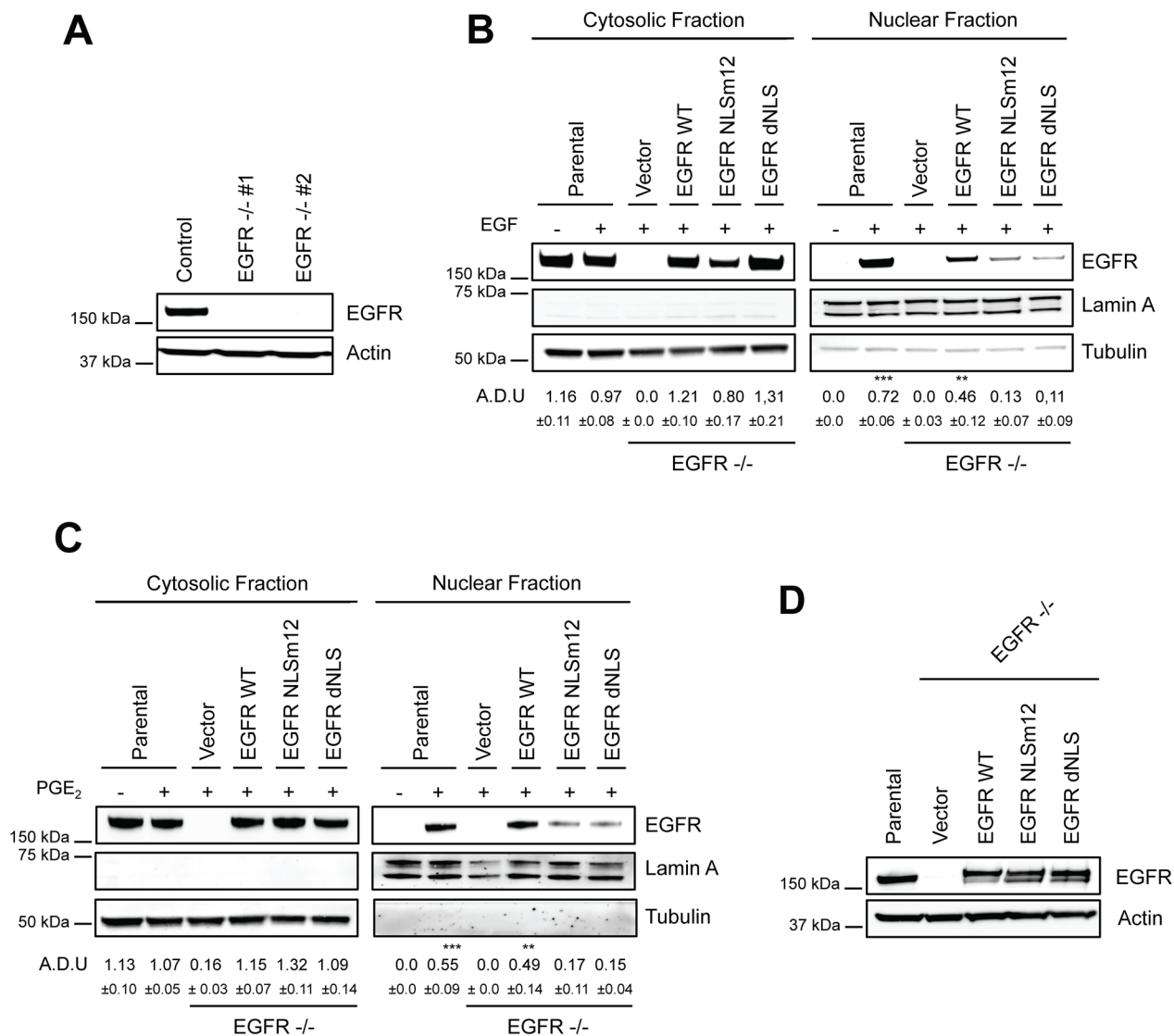
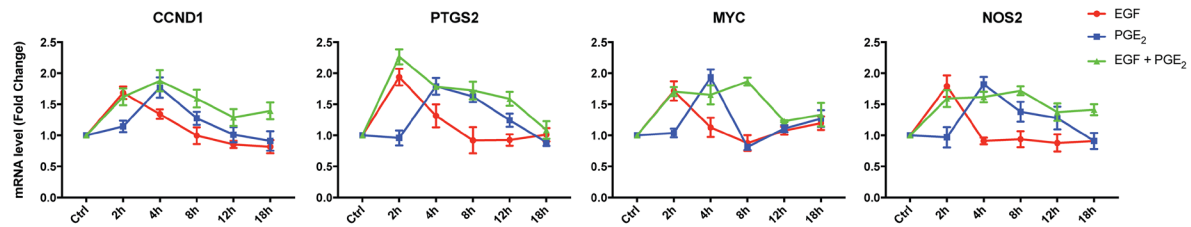
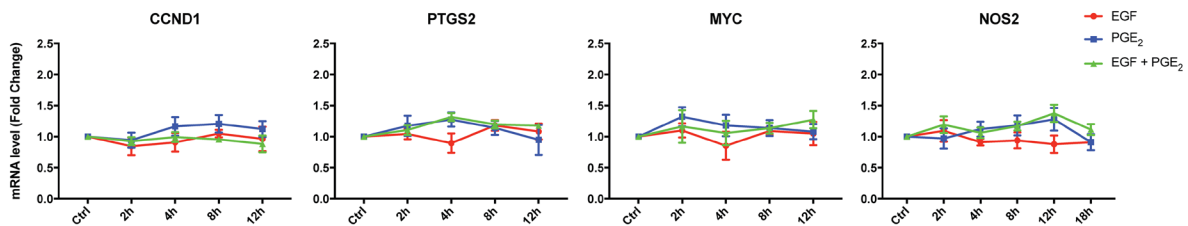


Figure 5: Generation and characterization of a model to study nuclear EGFR functions. (A) Immunoblotting analysis of EGFR expression in A549 wild type cells and two clones knockout for EGFR, generated by CRISPR/Cas9 (EGFR^{-/-} #1, #2). Actin was used as loading control. (B–C) EGFR knockout cells were transiently transfected with Vector or EGFR-WT or EGFR NLS mutant (NLSm12 or dNLS) plasmids for 48 h. Then EGFR nuclear import in response to 25 ng/ml EGF for 10 min (B) or to 1 μM PGE₂ for 60 min (C) was analyzed by immunoblotting upon cell fractionation. Parental cells were included as a control. Tubulin and Lamin A were used as loading control for cytosolic and nuclear fraction respectively. Immunoblotting quantification was expressed in A.D.U. (arbitrary density unit) and as mean ± SD. *p < 0.05, **p < 0.01, ***p < 0.001 vs Ctrl. EGFR in the cytoplasmic and nuclear fractions was normalized to Tubulin or Lamin A respectively. (D) Expression of EGFR in EGFR^{-/-} #1 cells, transfected with Vector, EGFR-WT and NLS mutant plasmids for 96 h. Actin was used as loading control. The experiments were performed three times.

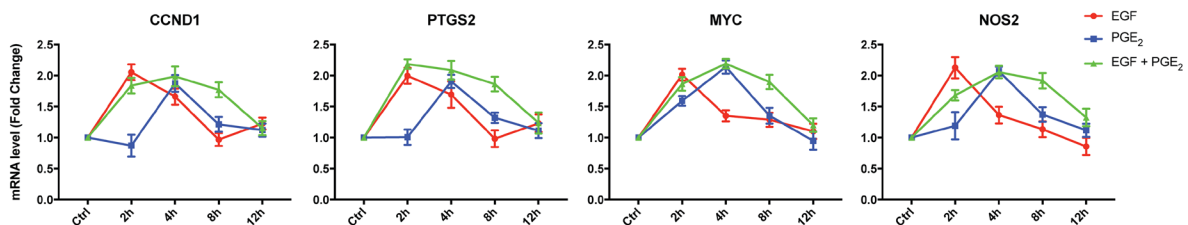
Parental Cells



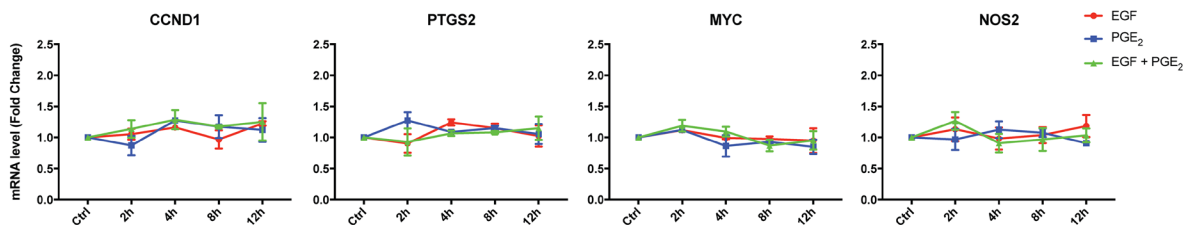
EGFR -/-



EGFR WT



EGFR NLS12



EGFR dNLS

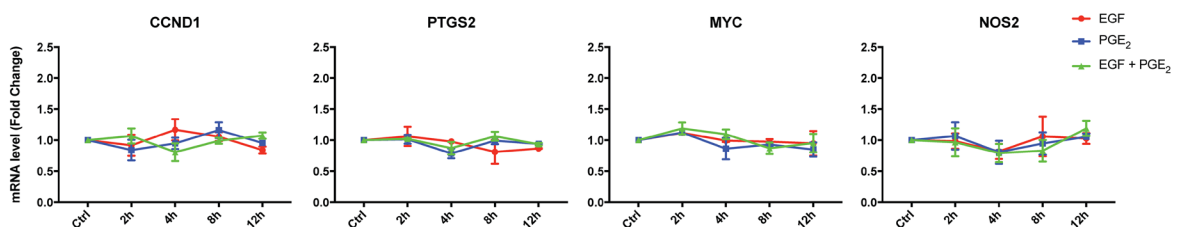


Figure 6: The combination of EGF and PGE₂ induces the transcription of nuclear EGFR gene signature up to 8 hours. Parental and modified A549 cells were starved overnight and then treated with 25 ng/ml EGF or 1 μ M PGE₂ or the combination for 2, 4, 8, 12, or 18 h. RNA was isolated and analyzed by qRT-PCR for a panel of nuclear EGFR target genes. The data are presented as mean of fold change \pm SD of three independent experiments, relative to non-treated cells (Control), which were assigned to 1. Statistical analysis is reported in Table 1 and Table 2. The experiments were performed three times.

Table 1: Statistical analysis of nuclear EGFR target genes regulated by EGF and PGE₂ in parental A549 cells

CCND1					
	2h	4h	8h	12h	18h
EGF vs Ctrl	0.0202 (*)	0.0479 (*)	0.9818 (ns)	0.1253 (ns)	0.2311 (ns)
PGE ₂ vs Ctrl	0.2561 (ns)	0.0422 (*)	0.1211 (ns)	0.9392 (ns)	0.6259 (ns)
EGF+PGE ₂ vs Ctrl	0.0447 (*)	0.0353 (*)	0.0493 (*)	0.2988 (ns)	0.101 (ns)
EGF+PGE ₂ vs EGF	0.731 (ns)	0.1028 (ns)	0.0924 (ns)	0.0983 (ns)	0.0795 (ns)
EGF+PGE ₂ vs PGE ₂	0.1013 (ns)	0.6912 (ns)	0.2138 (ns)	0.2659 (ns)	0.1448 (ns)
PTGS2					
	2h	4h	8h	12h	18h
EGF vs Ctrl	0.0197 (*)	0.2288 (ns)	0.7446 (ns)	0.5062 (ns)	0.9311 (ns)
PGE ₂ vs Ctrl	0.7688 (ns)	0.028 (*)	0.0205 (*)	0.1481 (ns)	0.1884 (ns)
EGF+PGE ₂ vs Ctrl	0.009 (**)	0.0013 (**)	0.0366 (*)	0.035 (*)	0.6021 (ns)
EGF+PGE ₂ vs EGF	0.2117 (ns)	0.1286 (ns)	0.0881 (ns)	0.045 (*)	0.7091 (ns)
EGF+PGE ₂ vs PGE ₂	0.0168 (*)	0.9534 (ns)	0.6262 (ns)	0.1562 (ns)	0.3235 (ns)
MYC					
	2h	4h	8h	12h	18h
EGF vs Ctrl	0.0441 (*)	0.4918 (ns)	0.4346 (ns)	0.3573 (ns)	0.2127 (ns)
PGE ₂ vs Ctrl	0.6387 (ns)	0.0181 (*)	0.0648 (ns)	0.1924 (ns)	0.182 (ns)
EGF+PGE ₂ vs Ctrl	0.0099 (**)	0.0478 (*)	0.0053 (**)	0.0038 (**)	0.2197 (ns)
EGF+PGE ₂ vs EGF	0.9568 (ns)	0.1388 (ns)	0.02 (*)	0.1441 (ns)	0.5973 (ns)
EGF+PGE ₂ vs PGE ₂	0.0112 (*)	0.296 (ns)	0.0058 (**)	0.1791 (ns)	0.8109 (ns)
NOS2					
	2h	4h	8h	12h	18h
EGF vs Ctrl	0.0448 (*)	0.2372 (ns)	0.6838 (ns)	0.4729 (ns)	0.1667 (ns)
PGE ₂ vs Ctrl	0.8677 (ns)	0.0208 (*)	0.1401 (ns)	0.265 (ns)	0.5583 (ns)
EGF+PGE ₂ vs Ctrl	0.0478 (*)	0.0184 (*)	0.0096 (**)	0.1155 (ns)	0.0421 (*)
EGF+PGE ₂ vs EGF	0.457 (ns)	0.0196 (*)	0.0337 (*)	0.1283 (ns)	0.0354 (*)
EGF+PGE ₂ vs PGE ₂	0.0982 (ns)	0.3008 (ns)	0.1936 (ns)	0.7193 (ns)	0.0835 (ns)

ns = non significant; * p < 0.05; ** p < 0.01.

even not statistically significant, between nuclear EGFR activity and poor prognosis in lung adenocarcinoma patients.

EGF and PGE₂ combination promotes NSCLC cell proliferation

To investigate whether the transcription of nuclear EGFR target genes-induced by the combination of EGF and PGE₂ could mediate and sustain NSCLC cell proliferation compared to single stimuli, the A549 EGFR-knockout cells described above were used. GLC82 cells knockout for EGFR were generated accordingly and

transfected with Empty Vector, or EGFR WT, or NLS mutant plasmids (Supplementary Figure 7A-7B). Similar level of EGFR expression was observed in A549 and GLC82 cells transfected with constructs encoding for WT and mutant (Figure 8A and Supplementary Figure 7C).

Specifically, we assessed whether the disruption of nuclear import of EGFR affected cancer cell proliferation. NSCLC cell proliferation was quantified by using a 5-bromo-2'-deoxy-uridine (BrdU) incorporation assay for 8-48 h (Figure 8B-8F and Supplementary Figure 7D-7H). In parental and EGFR WT expressing A549 cells, EGF and PGE₂ alone induced cell proliferation in a time-dependent manner with a peak at 16 h, declining toward

Table 2: Statistical analysis of nuclear EGFR target genes regulated by EGF and PGE₂ in EGFR knockout A549 cells bearing EGFR WT

<i>CCND1</i>				
	2h	4h	8h	12h
EGF vs Ctrl	0.0144(*)	0.0369(*)	0.7879(ns)	0.1404(ns)
PGE ₂ vs Ctrl	0.5417(ns)	0.0228(*)	0.2119(ns)	0.3722(ns)
EGF+PGE ₂ vs Ctrl	0.0220(*)	0.0247(*)	0.0236(*)	0.3111(ns)
EGF+PGE ₂ vs EGF	0.3542(ns)	0.2529(ns)	0.0368(*)	0.6618(ns)
EGF+PGE ₂ vs PGE ₂	0.0470(*)	0.6414(ns)	0.0497(*)	0.8610(ns)
<i>PTGS2</i>				
	2h	4h	8h	12h
EGF vs Ctrl	0.0162(*)	0.0824(ns)	0.9108(ns)	0.2415(ns)
PGE ₂ vs Ctrl	0.9602(ns)	0.0135(*)	0.0432(*)	0.2181(ns)
EGF+PGE ₂ vs Ctrl	0.0043(**)	0.0188(*)	0.0179(*)	0.2992(ns)
EGF+PGE ₂ vs EGF	0.3345(ns)	0.2700(ns)	0.0387(*)	0.9850(ns)
EGF+PGE ₂ vs PGE ₂	0.0150(*)	0.4289(ns)	0.0632(ns)	0.9204(*)
<i>MYC</i>				
	2h	4h	8h	12h
EGF vs Ctrl	0.0084(**)	0.0593(ns)	0.1278(ns)	0.4770(ns)
PGE ₂ vs Ctrl	0.0169(*)	0.0097(**)	0.1092(ns)	0.7608(ns)
EGF+PGE ₂ vs Ctrl	0.0156(*)	0.0042(**)	0.025(*)	0.2060(ns)
EGF+PGE ₂ vs EGF	0.4077(ns)	0.0194(*)	0.0485(*)	0.6039(ns)
EGF+PGE ₂ vs PGE ₂	0.1783(ns)	0.7295(ns)	0.0761(ns)	0.2999(ns)
<i>NOS2</i>				
	2h	4h	8h	12h
EGF vs Ctrl	0.0222(*)	0.1138(ns)	0.4012(ns)	0.4141(ns)
PGE ₂ vs Ctrl	0.4770(ns)	0.0043(**)	0.1694(ns)	0.3840(ns)
EGF+PGE ₂ vs Ctrl	0.0151(*)	0.0087(**)	0.0176(*)	0.1467(ns)
EGF+PGE ₂ vs EGF	0.1451(ns)	0.0534(ns)	0.0477(*)	0.1423(ns)
EGF+PGE ₂ vs PGE ₂	0.1716(ns)	0.9180(ns)	0.0452(*)	0.3600(ns)

ns = non significant; * p < 0.05; ** p < 0.01.

baseline at 36–48h. In cells exposed to a combination of EGF and PGE₂, BrdU incorporation levels increased at 16 h, doubled at 24 h and declined to baseline at 48 h, indicating that EGF and PGE₂ combination-induced nuclear EGFR sustained NSCLC cells growth (Figure 8B–8F). In contrast, cells expressing EGFR-NLS mutants were not comparably stimulated to proliferate in response to neither EGF nor PGE₂ (Figure 8B–8F). Similar results were obtained in GLC82 cells (Supplementary Figure 7D–7H). Statistical analysis has been reported in Table 3 and Supplementary Table 2 for A549 and GLC82 respectively.

In summary, we have identified the mechanisms by which PGE₂ promotes EGFR nuclear translocation in human NSCLC cells. PGE₂ internalizes EGFR through Clathrin and Caveolin- mediated endocytosis, whereas EGF preferentially promotes Clathrin-mediated EGFR internalization. Inside the cell, EGFR is imported to the nucleus by Importin β1 and associates with activated STAT3, and potentially other transcription factors, to induce the expression of nuclear EGFR target genes, thereby promoting cancer cell proliferation (Figure 9). The gene signature linked to EGFR nuclear internalization

in NSCLC cell lines matches that of patients with poor prognosis observed in patient with early stage NSCLC [37], suggesting a potential correlation with the clinical setting.

DISCUSSION

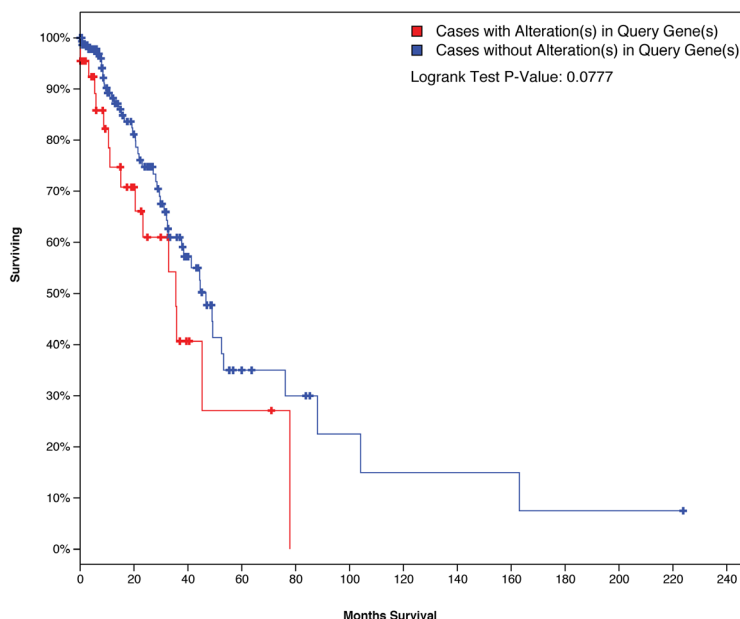
The inflammatory mediator PGE₂ is known to favor growth of several epithelial tumor cells in which the oncogenic drive is sustained by EGF/EGFR system. Two mechanisms are recognized as inducers of EGFR-mediated oncogenicity. The first one, occurring predominately at the cell membrane, consists in the activation of the receptor followed by a well-known effector cascade [38]. The second one involves EGFR internalization from the plasma membrane to the nucleus in which it serves as co-transcriptional factor [29, 39]. Recently, we dissected the mechanisms of PGE₂-mediated EGFR nuclear translocation showing marked differences in the

kinetic and in the internalization pattern between EGF and PGE₂ [12]. Here, we tested whether different endocytic mechanisms are involved in EGF and PGE₂-mediated EGFR nuclear translocation. Based on differences in time of induction and the internalization patterns, we hypothesized distinct mechanisms promoted by EGF or PGE₂.

EGFR is mainly internalized via Clathrin-mediated endocytosis [16] nevertheless, saturation of Clathrin or stimulation with different ligands could trigger alternative routes of internalization, including Caveolin-mediated endocytosis and macropinocytosis [17–19]. Using pharmacological inhibitors and siRNA targeting Clathrin heavy chain and Caveolin-1, we found that Clathrin knockdown abrogated EGFR nuclear translocation upon either EGF or PGE₂ treatment. However, Caveolin-1 knockdown or pharmacological inhibition (methyl- β -cyclodextrin (M β CD) suppressed solely PGE₂-mediated EGFR internalization (Figures 1–2, Supplementary

Case Set: Tumor Samples with mRNA data (RNA Seq V2) (230 patients / 230 samples)

Altered in 51 (22%) of 230 sequenced cases/patients (230 total)



	# Total Cases	# Cases Deceased	Median Months Survival
Cases with Alterations	44	16	35.5
Cases without Alterations	159	47	46.7

Figure 7: Bioinformatics analysis of nuclear EGFR gene signature in NSCLC patients using cBioPortal database. Alterations in nuclear EGFR target genes across TCGA provisional Lung adenocarcinoma samples analyzed by cBioPortal for cancer genomics database. Data were filtered for mRNA upregulation of nuclear EGFR target genes and the percentage on total samples was reported. Overall Survival Kaplan–Meier Estimate curve in lung adenocarcinoma patients with alteration (n= 44) or without alteration (n=159) in nuclear EGFR gene signature (Logrank Test P-Value: 0.0777). The table below the graph summarizes the total cases, deceased cases and median months survival data.

Figures 1–2). These findings demonstrate that Clathrin has a key role in EGFR internalization, whereas PGE₂ uses Caveolin as an alternative endocytic route to shuttle EGFR from the cell membrane to the nucleus. Notably, the uptake kinetics of Caveolin-mediated endocytosis is slower than that of Clathrin [40, 41], an observation that may explain the differences in the kinetics between EGF and PGE₂-mediated EGFR nuclear import. Moreover, we do not observe any enhancement in the modulation of PGE₂ activity on nuclear EGFR translocation when NSCLC cells were silenced for Clathrin heavy chain and Caveolin-1 together, suggesting that the two endocytic pathways activated by the prostanoid work independently (Supplementary Figure 3). However, we may not exclude that due to technical limitation, we could not discern the quantitative contribution of each individual endocytic routes.

As nuclear import of proteins bearing nuclear localization sequence (NLS) requires the interaction with Importin α/β for nuclear internalization [11], we show the key role of Importin β 1 in PGE₂-mediated EGFR nuclear translocation, as already reported for EGF (Figure 3).

Transcriptional regulation of genes involved in cell proliferation is one of the main functions of nuclear EGFR [39]. EGFR lacks a DNA binding domain and exerts its co-transcriptional functions via association with several transcription factors, including STAT3, STAT5 and E2F1 [42]. Among nuclear EGFR target genes, previously shown to be modulated by PGE₂ in NSCLC cells, *PTGS2*, *MYC* and *NOS2* have been shown to be induced by the EGFR-STAT3 complex [12, 31, 32, 34].

Based on these notions, we investigated whether PGE₂ leads to STAT3 activation and we found that the prostanoid promotes STAT3 phosphorylation with a peak

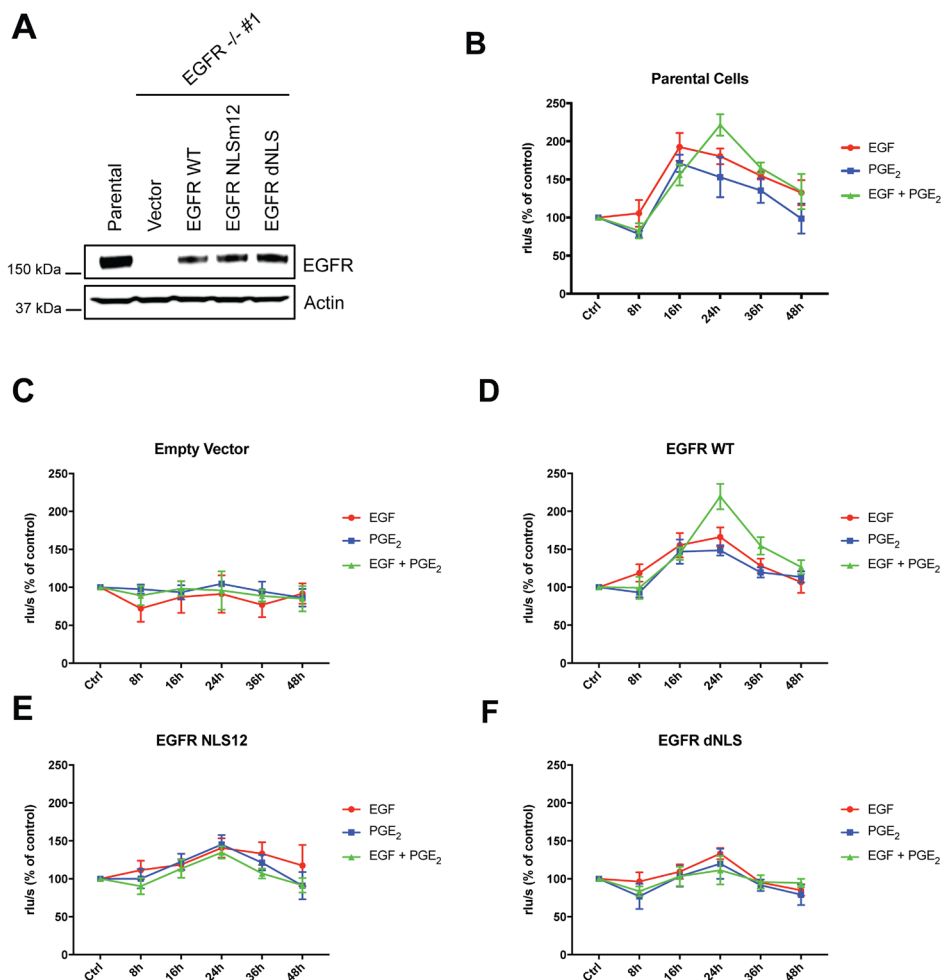


Figure 8: EGF and PGE₂ induce nuclear EGFR-mediated A549 cell proliferation. (A) Immunoblotting analysis of EGFR expression in A549 EGFR -/- #1 cells transfected with Vector, EGFR-WT and NLS mutant plasmids for 96 h. Parental cells were included as a control. Actin was used as loading control. (B–F) Parental cells or EGFR -/- #1, #2 cells transfected with Vector or EGFR WT or EGFR NLS12 or EGFR dNLS mutant plasmids for 24 h were harvested and seeded for BrdU incorporation assay. Cell proliferation was assessed by measuring the luminescence after 8, 16, 24, 36, 48 h treatment with EGF or PGE₂ or the combination. Data are mean \pm SD of triplicate cultures, expressed as % of control. Statistical analysis is reported in Table 3.

Table 3: Statistical analysis of BrdU incorporation assay performed in A549

Parental Cells					
	8h	16h	24h	36h	48h
EGF vs Ctrl	0.6082 (ns)	0.0009 (***)	0.0007 (***)	0.0005 (***)	0.026 (*)
PGE ₂ vs Ctrl	0.0012 (***)	0.0004 (***)	0.0251 (*)	0.0187 (*)	0.9111 (ns)
EGF+PGE ₂ vs Ctrl	0.0399 (*)	0.0021 (**)	0.0002 (***)	0.0001 (***)	0.0627 (ns)
EGF+PGE ₂ vs EGF	0.1207 (ns)	0.0493 (*)	0.0146 (*)	0.1148 (ns)	0.9314 (ns)
EGF+PGE ₂ vs PGE ₂	0.5137 (ns)	0.208 (ns)	0.0163 (*)	0.044 (*)	0.1124 (ns)
Empty Vector					
	8h	16h	24h	36h	48h
EGF vs Ctrl	0.0503 (ns)	0.3501 (ns)	0.5735 (ns)	0.0701 (ns)	0.3463 (ns)
PGE ₂ vs Ctrl	0.5394 (ns)	0.2854 (ns)	0.1136 (ns)	0.5076 (ns)	0.108 (ns)
EGF+PGE ₂ vs Ctrl	0.2124 (ns)	0.774 (ns)	0.7895 (ns)	0.0678 (ns)	0.1904 (ns)
EGF+PGE ₂ vs EGF	0.244 (ns)	0.4509 (ns)	0.8338 (ns)	0.3226 (ns)	0.6124 (ns)
EGF+PGE ₂ vs PGE ₂	0.3548 (ns)	0.5563 (ns)	0.5839 (ns)	0.544 (ns)	0.9156 (ns)
EGFR WT					
	8h	16h	24h	36h	48h
EGF vs Ctrl	0.0469 (*)	0.004 (**)	0.0008 (***)	0.0073 (**)	0.4643 (ns)
PGE ₂ vs Ctrl	0.1155 (ns)	0.007 (**)	0.0003 (***)	0.0071 (**)	0.0334 (*)
EGF+PGE ₂ vs Ctrl	0.936 (ns)	0.0007 (***)	0.0002 (***)	0.0012 (**)	0.0073 (**)
EGF+PGE ₂ vs EGF	0.1425 (ns)	0.3505 (ns)	0.0116 (*)	0.0382 (*)	0.1133 (ns)
EGF+PGE ₂ vs PGE ₂	0.5206 (ns)	0.8089 (ns)	0.0024 (**)	0.0104 (*)	0.1261 (ns)
EGFR NLS12					
	8h	16h	24h	36h	48h
EGF vs Ctrl	0.1777 (ns)	0.0113 (*)	0.0121 (*)	0.0189 (*)	0.3301 (ns)
PGE ₂ vs Ctrl	0.9847 (ns)	0.0199 (*)	0.0183 (*)	0.0177 (*)	0.4278 (ns)
EGF+PGE ₂ vs Ctrl	0.1889 (ns)	0.1268 (ns)	0.0016 (**)	0.1341 (ns)	0.1984 (ns)
EGF+PGE ₂ vs EGF	0.0856 (ns)	0.5404 (ns)	0.1505 (ns)	0.0517 (ns)	0.1943 (ns)
EGF+PGE ₂ vs PGE ₂	0.363 (ns)	0.3641 (ns)	0.1791 (ns)	0.1107 (ns)	0.9641 (ns)
EGFR dNLS					
	8h	16h	24h	36h	48h
EGF vs Ctrl	0.6342 (ns)	0.1039 (ns)	0.0015 (**)	0.043 (*)	0.0232 (*)
PGE ₂ vs Ctrl	0.116 (ns)	0.0482 (*)	0.1585 (ns)	0.1676 (ns)	0.1562 (ns)
EGF+PGE ₂ vs Ctrl	0.0122 (*)	0.6773 (ns)	0.352 (ns)	0.4671 (ns)	0.1562 (ns)
EGF+PGE ₂ vs EGF	0.1783 (ns)	0.5399 (ns)	0.1325 (ns)	0.9016 (ns)	0.1454 (ns)
EGF+PGE ₂ vs PGE ₂	0.7811 (ns)	0.4621 (ns)	0.1999 (ns)	0.7544 (ns)	0.0531 (ns)

ns = non significant; * p < 0.05; ** p < 0.01; *** p < 0.001.

at 30 min (Figure 4A). Upstream to STAT3 activation mediated by PGE₂, JAK activity appears to be required, as its inhibition significantly reduced PGE₂-mediated

activity (Figure 4B). We have assessed a direct EGFR-STAT3 interaction by co-immunoprecipitation and find that STAT3, in both non-phosphorylated and phosphorylated

conditions, physically associates and colocalizes with EGFR following PGE₂ treatment (Figure 4C–4E). Moreover, Caveolin-1 knockdown affected PGE₂-mediated EGFR-STAT3 association, highlighting the functional role of Caveolin endocytosis in PGE₂ activity. (Figure 4F–4G and Supplementary Figures 4 and 5).

By analyzing the expression of target genes of nuclear EGFR in NSCLC cells, we found that *CCND1*, *PTGS2*, *MYC* and *NOS2* mRNA levels were upregulated by EGF as well as by PGE₂, yet with different kinetics indicating the involvement of distinct internalization pathways (Figure 6 and Supplementary Figure 6). Interestingly, the combination of treatments induced a prolonged transcriptional activation of nuclear EGFR gene signature compared to individual stimuli (from 2–4 to 8h), indicating that the PGE₂ and EGF cooperate in their

activities to sustain tumor progression. Additionally, by using cBioPortal for Cancer Genomics database, we have found a reduction in median months of survival in lung cancer patients that exhibit an upregulation of a nuclear EGFR gene signature, thus showing a trend between nuclear EGFR and poor prognosis in NSCLC (Figure 7). It is worth to mention that these data were derived from a non-selected patient population characterized by large differences in: age, sex, tumor stage, smoking history and therapy, therefore representing a heterogeneous situation. Among nuclear EGFR target genes, *MYC* is of high prognostic value in different epithelial tumors [43], and its expression is driven by PGE₂ in NSLC cells [44]. Further, *MYC* appears to be one of the most amplified genes across nuclear EGFR transcriptional signature, further corroborating our findings.

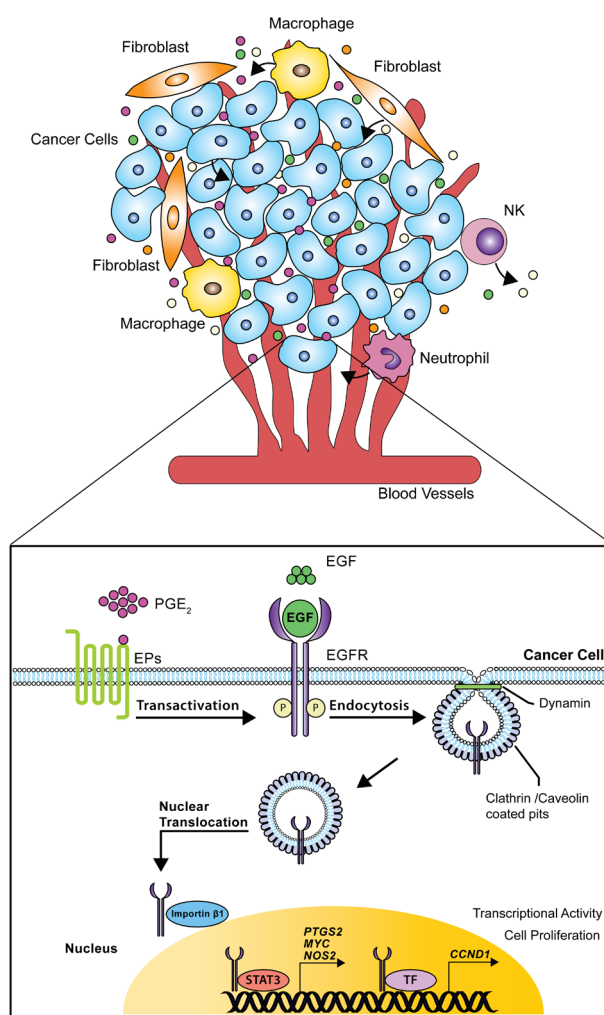


Figure 9: Schematic model of nuclear EGFR signaling in NSCLC cells. The tumor microenvironment consists in cancer cells surrounded by different cell types such as stromal, endothelial, inflammatory and immune cells. In this scenario, single entities release mediators, cytokines and growth factors thereby supporting tumor progression. Particularly, EGF and PGE₂ activate or transactivate EGFR leading to its internalization via dynamin-dependent Clathrin and Caveolin endocytosis. Further, Importin β1 transports the NLS-bearing EGFR across the nuclear envelope to the nucleoplasm. Within the nucleus, EGFR interacts with STAT3 or other transcription factors (TF) promoting the transcription of *CCND1*, *PTGS2*, *MYC* and *NOS*, a process that culminates with increased tumor cell proliferation.

To demonstrate that tumor gene reprogramming promoted by EGF and PGE₂-induced nuclear EGFR is critical for tumor progression, we have assessed cell proliferation by BrdU incorporation assay in NSCLC cells. A549 and GLC82 EGFR knockout cells expressing wild type EGFR increase in their proliferation in response to PGE₂ or EGF in contrast to cells transfected with mutant EGFR into its nuclear localization sequence (Figure 8B–8F and Supplementary Figure 7D–7H). Notably, the combined treatment potentiates nuclear EGFR mitogenic activity in terms of time and intensity, supporting the hypothesis of EGF and PGE₂ malignant alliance.

In this scenario, we identified PGE₂ as an inducer of EGFR nuclear translocation in NSCLC cells, an event, which has clinical correlate with poor prognosis [44, 45]. PGE₂ coupling with EP receptor triggers EGFR internalization. In particular, we showed that EGFR undergoes to Clathrin- and Caveolin-mediated endocytosis leading to association with Importin β 1 and consequent nuclear import. Within the nucleus, EGFR interacts with transcription factors such as STAT3 to regulate gene expression. Particularly, nuclear EGFR induced by EGF or PGE₂ or the combination of treatments, promotes *CCND1*, *PTGS2*, *MYC* and *NOS2* upregulation and sustains tumor growth (Figure 9), supporting the hypothesis that the gene signature associated with nuclear EGFR is correlated with poor prognosis in NSCLC and may serve as a biomarker for patients outcome and treatment selection.

Collectively, the findings of this work on EGFR nuclear import and gene transcription, assume the character of a self-feeding loop which leads to persistent up-regulation of *CCND1*, *PTGS2*, *NOS2* and *MYC*, hence overproduction of PGE₂, NO and overload of MYC which support a favorable pro-tumor microenvironment.

MATERIALS AND METHODS

Cell culture and cultured conditions

The human NSCLC cancer cell line A549 (CCL-185), was purchased from American Type Culture Collection and the GLC82 NSCLC cell line was kindly provided by Dr. Mario Chiariello (Istituto Toscano Tumori, Siena, Italy). Cells were certified by STRA, (LGC Standards S.r.l., Sesto San Giovanni, Milan, Italy) and were cultured in DMEM for A549 and in RPMI-1640 (Euroclone, Milan, Italy) for GLC82 supplemented with 10% FBS and 2 mM Glutamine, 100 Units Penicillin and 0.1mg/l Streptomycin (Sigma Aldrich, St. Louis, MO, USA) in a humidified incubator with 5% CO₂ at 37°C. A549 and GLC82 were immediately expanded after delivery (up to 6 × 10⁷ cells) and frozen down (1 × 10⁶ per vial) such that both cell lines could be restarted after a maximum of 10 passages every 3 months from a frozen vial of the same batch of cells. Control of mycoplasma was performed regularly using MycoAlert™ PLUS

Mycoplasma Decection Kit (#LT07-710 Lonza, Basel, Switzerland).

Chemicals and reagents

Recombinant human EGF (#AF-100-15) was purchased from PeproTech (Rocky Hill, NJ, USA). PGE₂ (#P0409), Dynasore (#D7693), 5-N-Ethyl-N-isopropyl amiloride (EIPA) (#A3085) and Metil beta cyclodextrin (#C4555,) were purchased from Sigma Aldrich. Ruxolitinib (#S1378) was purchased from Selleckchem (Houston, TX, USA). STAT3 Inhibitor VII Calbiochem (#573103) was purchased from Merck Millipore (Darmstadt, Germany).

Antibodies

Anti-EGFR (#4267), anti-STAT3 (#9139), anti-pSTAT3 Tyr 705 (#9138), anti-Caveolin-1 (#3267), anti-Clathrin Heavy Chain (#4796), anti-Importin- β 1 (#8673) antibodies were purchased from Cell Signaling Technology (Danvers, MA, USA). Anti-Tubulin antibody (#T9026) was purchased from Santa Cruz (Heidelberg, Germany). Anti-Lamin A (#SAB4501764), anti-Actin (#A5441) antibodies were obtained from Sigma Aldrich.

Whole cell extracts

Cells were washed 2x with cold Dulbecco's Phosphate Buffered Saline (Sigma Aldrich) and lysed on ice with CellLytic™ MT Cell Lysis Reagent (#C3228 Sigma Aldrich) supplemented with 2mM Na₃VO₄ and 1x Protease inhibitor cocktail for mammalian cells (#P2714 Sigma Aldrich). Cell lysates were centrifuged at 16000 × g for 20 min at 4°C and the supernatants were then collected for immunoblot.

Cell fractionation

Nuclear and cytoplasmic extracts were prepared with NE-PER™ (#78833) nuclear and cytoplasmic extraction reagents (ThermoFisher Scientific, Waltham, MA, USA) following the manufacturer's instructions as described previously [11].

Immunoblotting analysis

4 × 10⁵ cells were plated in 60 mm dishes, serum deprived (0.1% fetal calf serum, overnight), then treated as described in the text. Protein concentration was determined using the BCA protein assay kit (#23227 ThermoFisher Scientific). For whole cell lysates, an equal amount of proteins were loaded on SDS–polyacrylamide gel and then transferred to a nitrocellulose membrane (#10600002 GE Healthcare Lifesciences) For cell fractionation experiments, 10 μ g of the cytosolic and 40 μ g of the nuclear extracts were applied for SDS-

PAGE. Immunoblot analysis was performed as described previously [8, 10]. Signals were detected by SuperSignal WestPico Chemiluminescent Substrate (#34578 ThermoFisher Scientific) using ChemiDoc system and Quantity one software (Bio-Rad, Hercules, CA, USA). All experiments were performed at least three times. For all experiments using whole cell lysate, Actin was used as loading control. Lamin-A and Tubulin were used as loading and purity controls for the nuclear and cytosolic fractions, respectively. Immunoblots were analyzed by densitometry using NIH Image J 1.48v software, and the results, expressed as arbitrary density units (A.D.U.) \pm SD, were normalized to Actin, EGFR, STAT3, Lamin-A or Tubulin.

Immunofluorescence microscopy analysis

Cells were plated on glass coverslips, starved overnight and treated as described in the text. Cells were fixed using 4% paraformaldehyde/PBS for 15 min and permeabilized with 0.5% NP-40 for 5 min. Next, cells were blocked using 3% BSA, 0.01% TritonX-100 in PBS for 20 min. Furthermore, cells were incubated with anti-EGFR, overnight at 4°C followed by 3x washes with PBS/ 0.01% TritonX-100 and incubation with the AlexaFluor® 488-labeled (#A11034 Invitrogen, Carlsbad, CA, USA) for 60 min at room temperature. After 3x washes with PBS/ 0.01% TritonX-100, nuclei were stained with 6-diamidino-2- phenylindole (DAPI #D9542) or propidium iodide (PI #P4864) 1 μ g/ml (Sigma Aldrich) for 20 min. The coverslips were mounted with fluorescent mounting medium (#S3023 Dako, Glostrup, Denmark) on microscope slides. Cells were analyzed with a confocal laser scanning microscope Leica SP5. Images for documenting EGFR nuclear translocation and colocalization with Caveolin-1 were acquired in the middle section of the nuclei with 63x magnification.

Transfection of siRNAs and plasmids

siRNAs used for transient knock-down experiments were purchased from Qiagen (Hilden, Germany). Cells were transfected with 20nM targeting siRNA or scrambled control siRNA using Lipofectamine® RNAiMAX (#13778150 Invitrogen) according to manufacturer's instructions. Cells were assayed 48-72h after transfection. Knockdown efficiency was assessed by immunoblotting. Target sequences are listed in Supplementary Table 3.

For DNA transfection, cells were transfected with 1–10 μ g plasmid using Lipofectamine® 2000 (#12566014 Invitrogen) according to manufacturer's instructions. EGFR WT and NLS mutant plasmids (NLSm12 and dNLS) were kindly provided by Prof. Mien-Chie Hung (University of Texas MD Anderson Cancer Center, Houston, TX, USA) [32]. pSpCas9(BB)-2A-GFP (PX458) (#48138) was purchased from Addgene. Cells were analyzed 24–96 h post-transfection.

Knockout of EGFR by CRISPR/Cas9-mediated genome editing

A549 and GLC82 EGFR knockout cells were generated by CRISPR/Cas9 as previously described [12].

Immunoprecipitation

1 \times 10⁶ were plated in 100 mm diameter dishes and starved overnight in 0.1% FBS. Then, cells were treated according to experimental design and lysed with CelLytic™ MT Cell Lysis Reagent (Sigma Aldrich) or subjected to cell fractionation with NE-PER™ nuclear and cytoplasmic extraction reagents (ThermoFisher Scientific). 300 μ g of total proteins per sample were immunoprecipitated using Dynabeads™ Protein G Immunoprecipitation Kit (#10007D ThermoFisher Scientific) with an Anti-EGFR antibody (#4267 Cell signaling) following the manufacturer's instructions. Immunoprecipitates were solubilized in LDS Sample Buffer (#NP0007 ThermoFisher Scientific) supplemented with Sample reducing agent (#NP0004 ThermoFisher Scientific), boiled for 10 min, separated in SDS/4-12% polyacrylamide gel and transferred onto nitrocellulose membranes. Immunoblotting analysis was performed using anti-STAT3 (#9139 Cell signaling) or anti-pSTAT3 Tyr 705 (#9138 Cell signaling) antibodies.

Real time PCR

Total RNA was prepared using RNeasy Plus Kit (#74134 Qiagen) following manufacturer's instructions. 1 μ g RNA was reverse transcribed using QuantiTect Reverse Transcription Kit (# 205313 Qiagen) and quantitative RT-PCR was performed using QuantiNova SYBR Green PCR Kit (#208056 Qiagen) in a Rotor-Gene Q PCR machine (Qiagen). Fold change expression was determined by the comparative Ct method ($\Delta\Delta$ Ct) normalized to 60S Ribosomal protein L19 expression. qRT-PCR data are represented as fold increase relative to non-treated cells (Control), which were assigned to 1. Primers for quantitative RT-PCR are listed in Supplementary Table 4.

Analysis of nuclear EGFR gene signature in TCGA provisional lung adenocarcinoma samples

cBioPortal for Cancer Genomics dataset (<http://cbioportal.org>) was used to analyze the nuclear EGFR target gene signature, which consists of *CCND1*, *PTGS2*, *MYC* and *NOS2* mRNA upregulation in lung adenocarcinoma TCGA study that includes 230 sequenced samples [35, 36]. The summary of mRNA upregulation of nuclear EGFR target genes across tumor samples reported in the text was generated using OncoPrint view. The available survival data are displayed as Kaplan-Meier plots with P values derived from a logrank test.

BrdU incorporation assay

Cell proliferation was determined by 5-bromo-2'-deoxy-uridine (BrdU) incorporation using a chemiluminescence ELISA according to the manufacturer's instructions (#11669915001 Roche Diagnostic S.p.A, Monza, Italy). Briefly, 3×10^3 cells were seeded in 96-well plate and starved overnight in growth medium 0.1% FBS. Next, cells were exposed to 5ng/ml EGF or 1 μ M PGE₂ or combination of treatments for 8, 16, 24, 36 and 48 h. BrdU was added during the late stage (8 h) of incubation. Then, cells were processed following manufacturer's protocol. Chemiluminescence generated by BrdU labelled cells was measured using Infinite F200 Pro luminometer (Tecan life sciences, Switzerland). Data are reported as % relative to non-treated cells.

Statistical analysis

Statistical analysis and graphs were generated using the GraphPad Prism software (San Diego, CA, USA). All statistical analysis was done by unpaired/paired Student's *t*-test, *p*-value < 0.05 was considered significant.

Abbreviations

A.D.U: Arbitrary density unit; ADAM: A disintegrin and metalloproteinase; BrdU: 5-bromo-2'-deoxy-uridine; CCND1: Cyclin D1; CIE: Clathrin-independent endocytosis; CME: Clathrin-mediated endocytosis; DAPI: 4',6-diamidino-2-phenylindole; DYN: Dynasore; E2F1: Retinoblastoma-Associated Protein 1; EGF: Epidermal growth factor; EGFR: Epidermal growth factor receptor; EIPA: 5-N-Ethyl-N-isopropyl amiloride; JAK: Janus Kinase; MYC: c-Myc; M β CD: Methyl- β -cyclodextrin; NLS: Nuclear localization sequence; NOS2: Inducible Nitric oxide synthase; NSCLC: Non-small cell lung cancer; PGE2: Prostaglandin E2; PI3K: Phosphatidylinositol-4,5-Bisphosphate 3-Kinase; PKA: Protein kinase A; PKC: Protein kinase C; PTGS2: Cyclooxygenase 2; qRT-PCR: Quantitative Real Time PCR; SD: Standard deviation; siRNA: Small interfering RNA; SRC: V-Src Avian Sarcoma (Schmidt-Ruppin A-2) Viral Oncogene; STAT3: Signal transducer and activator of transcription 3; STAT5: Signal transducer and activator of transcription 5; TCGA: The cancer genome atlas; WT: Wild Type.

Author contributions

LB participated in designing the study, performed the experiments, analyzed the data and wrote the manuscript; SD participated in designing the study, analyzed the data and wrote the manuscript; AG supervised the study, wrote and reviewed the manuscript; GC supervised the study, analyzed the data and reviewed the manuscript; MZ

designed the study, oversaw and analyzed the experiments, wrote and reviewed the manuscript.

ACKNOWLEDGMENTS

We thank Pascal Lorentz (BioOptics Facility, Department of Biomedicine, University of Basel, Switzerland) for support with confocal microscopy. We are grateful to Prof. Mien-Chie Hung (MD Anderson Cancer Center, University of Texas, USA) for providing EGFR plasmids and to Dr. Mario Chiariello (Istituto Toscano Tumori, Italy) for GLC82 cells.

CONFLICTS OF INTEREST

The authors declare no conflicts of interest.

FUNDING

This work was supported by Associazione Italiana per la Ricerca sul Cancro (AIRC) IG15443, MIUR-PRIN (2015SHKF32), Progetto Omiterc - Bando FAS Salute 2014, the Swiss National Science Foundation (310030B-163471) and the Swiss Cancer League (KFS-3479-08-2014).

REFERENCES

1. Ziche M, Jones J, Gullino PM. Role of prostaglandin E1 and copper in angiogenesis. *J Natl Cancer Inst.* 1982; 69:475–482.
2. Wang D, Dubois RN. Eicosanoids and cancer. *Nat Rev Cancer.* 2010; 10:181–193.
3. Narumiya S, Sugimoto Y, Ushikubi F. Prostanoid receptors: structures, properties, and functions. *Physiol Rev.* 1999; 79:1193–1226.
4. Cattaneo F, Guerra G, Parisi M, De Marinis M, Tafuri D, Cinelli M, Ammendola R. Cell-surface receptors transactivation mediated by G protein-coupled receptors. *Int J Mol Sci.* 2014; 15:19700–19728.
5. Finetti F, Terzuoli E, Giachetti A, Santi R, Villari D, Hanaka H, Radmark O, Ziche M, Donnini S. mPGES-1 in prostate cancer controls stemness and amplifies epidermal growth factor receptor-driven oncogenicity. *Endocr Relat Cancer.* 2015; 22:665–678.
6. Fernandez-Martinez AB, Lucio Cazana FJ. Epidermal growth factor receptor transactivation by intracellular prostaglandin E2-activated prostaglandin E2 receptors. Role in retinoic acid receptor-beta up-regulation. *Biochim Biophys Acta.* 2013; 1833:2029–2038.
7. Donnini S, Finetti F, Terzuoli E, Giachetti A, Iniguez MA, Hanaka H, Fresno M, Radmark O, Ziche M. EGFR signaling upregulates expression of microsomal prostaglandin E synthase-1 in cancer cells leading to enhanced tumorigenicity. *Oncogene.* 2012; 31:3457–3466.

8. Donnini S, Finetti F, Solito R, Terzuoli E, Sacchetti A, Morbidelli L, Patrignani P, Ziche M. EP2 prostanoid receptor promotes squamous cell carcinoma growth through epidermal growth factor receptor transactivation and iNOS and ERK1/2 pathways. *FASEB J*. 2007; 21:2418–2430.
9. Buchanan FG, Wang D, Bargiacchi F, DuBois RN. Prostaglandin E2 regulates cell migration via the intracellular activation of the epidermal growth factor receptor. *J Biol Chem*. 2003; 278:35451–35457.
10. Corti F, Finetti F, Ziche M, Simons M. The syndecan-4/protein kinase alpha pathway mediates prostaglandin E2-induced extracellular regulated kinase (ERK) activation in endothelial cells and angiogenesis *in vivo*. *J Biol Chem*. 2013; 288:12712–12721.
11. Lappano R, Maggiolini M. G protein-coupled receptors: novel targets for drug discovery in cancer. *Nat Rev Drug Discov*. 2011; 10:47–60.
12. Bazzani L, Donnini S, Finetti F, Christofori G, Ziche M. PGE2/EP3/SRC signaling induces EGFR nuclear translocation and growth through EGFR ligands release in lung adenocarcinoma cells. *Oncotarget*. 2017; 8:31270–31287. <https://doi.org/10.18632/oncotarget.16116>.
13. Wang Y, Pennock S, Chen X, Wang Z. Endosomal signaling of epidermal growth factor receptor stimulates signal transduction pathways leading to cell survival. *Mol Cell Biol*. 2002; 22:7279–7290.
14. Sorkin A, von Zastrow M. Endocytosis and signalling: intertwining molecular networks. *Nat Rev Mol Cell Biol*. 2009; 10:609–622.
15. Le Roy C, Wrana JL. Clathrin- and non-clathrin-mediated endocytic regulation of cell signalling. *Nat Rev Mol Cell Biol*. 2005; 6:112–126.
16. Sigismund S, Argenzio E, Tosoni D, Cavallaro E, Polo S, Di Fiore PP. Clathrin-mediated internalization is essential for sustained EGFR signaling but dispensable for degradation. *Dev Cell*. 2008; 15:209–219.
17. Sigismund S, Woelk T, Puri C, Maspero E, Tacchetti C, Transidico P, Di Fiore PP, Polo S. Clathrin-independent endocytosis of ubiquitinated cargos. *Proc Natl Acad Sci USA*. 2005; 102:2760–65.
18. Orth JD, Krueger EW, Weller SG, McNiven MA. A novel endocytic mechanism of epidermal growth factor receptor sequestration and internalization. *Cancer Res*. 2006; 66:3603–3610.
19. Henriksen L, Grandal MV, Knudsen SL, van Deurs B, Grovdal LM. Internalization mechanisms of the epidermal growth factor receptor after activation with different ligands. *PLoS One*. 2013; 8:e58148.
20. Mayor S, Pagano RE. Pathways of clathrin-independent endocytosis. *Nat Rev Mol Cell Biol*. 2007; 8:603–612.
21. Ferguson SM, De Camilli P. Dynamin, a membrane-remodelling GTPase. *Nat Rev Mol Cell Biol*. 2012; 13:75–88.
22. Koivusalo M, Welch C, Hayashi H, Scott CC, Kim M, Alexander T, Touret N, Hahn KM, Grinstein S. Amiloride inhibits macropinocytosis by lowering submembranous pH and preventing Rac1 and Cdc42 signaling. *J Cell Biol*. 2010; 188:547–563.
23. McMahon HT, Boucrot E. Molecular mechanism and physiological functions of clathrin-mediated endocytosis. *Nat Rev Mol Cell Biol*. 2011; 12:517–533.
24. Parton RG, Simons K. The multiple faces of caveolae. *Nat Rev Mol Cell Biol*. 2007; 8:185–194.
25. Rodal SK, Skretting G, Garred O, Vilhardt F, van Deurs B, Sandvig K. Extraction of cholesterol with methyl-beta-cyclodextrin perturbs formation of clathrin-coated endocytic vesicles. *Mol Biol Cell*. 1999; 10:961–974.
26. Lott K, Cingolani G. The importin beta binding domain as a master regulator of nucleocytoplasmic transport. *Biochim Biophys Acta*. 2011; 1813:1578–1592.
27. Hsu SC, Hung MC. Characterization of a novel tripartite nuclear localization sequence in the EGFR family. *J Biol Chem*. 2007; 282:10432–10440.
28. Lo HW, Ali-Seyed M, Wu Y, Bartholomeusz G, Hsu SC, Hung MC. Nuclear-cytoplasmic transport of EGFR involves receptor endocytosis, importin beta1 and CRM1. *J Cell Biochem*. 2006; 98:1570–1583.
29. Brand TM, Iida M, Li C, Wheeler DL. The nuclear epidermal growth factor receptor signaling network and its role in cancer. *Discov Med*. 2011; 12:419–432.
30. Lo HW, Hung MC. Nuclear EGFR signalling network in cancers: linking egfr pathway to cell cycle progression, nitric oxide pathway and patient survival. *Br J Cancer*. 2006; 94:184–188.
31. Lo HW, Hsu SC, Ali-Seyed M, Gunduz M, Xia W, Wei Y, Bartholomeusz G, Shih JY, Hung MC. Nuclear interaction of EGFR and STAT3 in the activation of the iNOS/No pathway. *Cancer Cell*. 2005; 7:575–589.
32. Lo HW, Cao X, Zhu H, Ali-Osman F. Cyclooxygenase-2 is a novel transcriptional target of the nuclear EGFR-STAT3 and EGFRvIII-STAT3 signaling axes. *Mol Cancer Res*. 2010; 8:232–245.
33. Lin SY, Makino K, Xia W, Matin A, Wen Y, Kwong KY, Bourguignon L, Hung MC. Nuclear localization of EGF receptor and its potential new role as a transcription factor. *Nat Cell Biol*. 2001; 3:802–808.
34. Jaganathan S, Yue P, Paladino DC, Bogdanovic J, Huo Q, Turkson J. A functional nuclear epidermal growth factor receptor, SRC and Stat3 heteromeric complex in pancreatic cancer cells. *PLoS One*. 2011; 6:e19605.
35. Gao J, Aksoy BA, Dogrusoz U, Dresdner G, Gross B, Sumer SO, Sun Y, Jacobsen A, Sinha R, Larsson E, Cerami E, Sander C, Schultz N. Integrative analysis of complex cancer genomics and clinical profiles using the cBioPortal. *Sci Signal*. 2013; 6:p11.
36. Cerami E, Gao J, Dogrusoz U, Gross BE, Sumer SO, Aksoy BA, Jacobsen A, Byrne CJ, Heuer ML, Larsson E, Antipin Y, Reva B, Goldberg AP, et al. The cBio cancer genomics portal: an open platform for exploring

- multidimensional cancer genomics data. *Cancer Discov.* 2012; 2:401–404.
37. Traynor AM, Weigel TL, Oettel KR, Yang DT, Zhang C, Kim K, Salgia R, Iida M, Brand TM, Hoang T, Campbell TC, Hernan HR, Wheeler DL. Nuclear EGFR protein expression predicts poor survival in early stage non-small cell lung cancer. *Lung Cancer.* 2013; 81:138–141.
 38. Citri A, Yarden Y. EGF-ERBB signalling: towards the systems level. *Nat Rev Mol Cell Biol.* 2006; 7:505–516.
 39. Lee HH, Wang YN, Hung MC. Non-canonical signaling mode of the epidermal growth factor receptor family. *Am J Cancer Res.* 2015; 5:2944–2958.
 40. Tran D, Carpentier JL, Sawano F, Gorden P, Orci L. Ligands internalized through coated or noncoated invaginations follow a common intracellular pathway. *Proc Natl Acad Sci USA.* 1987; 84:7957–61.
 41. Rejman J, Bragonzi A, Conese M. Role of clathrin- and caveolae-mediated endocytosis in gene transfer mediated by lipo- and polyplexes. *Mol Ther.* 2005; 12:468–474.
 42. Brand TM, Iida M, Luthar N, Starr MM, Huppert EJ, Wheeler DL. Nuclear EGFR as a molecular target in cancer. *Radiother Oncol.* 2013; 108:370–377.
 43. Wolfer A, Ramaswamy S. MYC and metastasis. *Cancer Res.* 2011; 71:2034–2037.
 44. Krysan K, Kusko R, Grogan T, O’Hearn J, Reckamp KL, Walser TC, Garon EB, Lenburg ME, Sharma S, Spira AE, Elashoff D, Dubinett SM. PGE2-driven expression of c-Myc and oncomir-17-92 contributes to apoptosis resistance in NSCLC. *Mol Cancer Res.* 2014; 12:765–774.
 45. Nakanishi M, Rosenberg DW. Multifaceted roles of PGE2 in inflammation and cancer. *Semin Immunopathol.* 2013; 35:123–137.